International Journal of Mechanical, Industrial and Aerospace Sciences
ISSN: 2517-9950
Vol:5, No:6, 2011

Effects of various substrate openings for electronic cooling under forced and natural convection

Shen-Kuei Du, Jen-Chieh Chang, Chia-Hong Kao, Tzu-Chen Hung, Chii-Ray Lin

***Abstract*—**This study experimentally investigates the heat transfer effects of forced convection and natural convection under different substrate openings design. A computational fluid dynamics (CFD) model was established and implemented to verify and explain the experimental results and heat transfer behavior. It is found that different opening position will destroy the growth of the boundary layer on substrates to alter the cooling ability for both forced under low Reynolds number and natural convection. Nevertheless, having too many opening may reduce heat conduction and affect the overall heat transfer performance. This study provides future researchers with a guideline on designing and electronic package manufacturing.

***Keywords*—**electronic cooling, experiment, opening concept, CFD.

I. Introduction

ELECTRONIC devices have been developed with a trend toward higher performance and smaller dimensions. These electronic devices normally contain a fairly high energy density. When used for an extensive amount of time, it can shorten the life span of a device and increase the difficulty of packaging the product. It is vital to remove the heat of an electronic chip when it comes to its design and manufacture. Moreover, the material, thermal resistance and circuit design are all crucial factors to the temperature of the chip. For instance, the reliability of a silicon chip is decreased by about 10% for every 2K temperature rise [1]. In Yeh`s review paper [2], a U.S. Air Force study indicated that more than 50% of the electronic failures are temperature-related. Therefore, several methods have been employed to improve electronic devices temperature in recent years.

Forced convection have been widely reviewed [3] and studied and generally offer higher power dissipation capabilities than natural convection systems. A series of experimental investigations with array configurations have been carried out by Sparrow et al. [4-6] and Moffat et al. [7]. Three-dimensional laminar and turbulent heat transfer analyses of these configurations of problems were investigated by Faghri and Asako [8]. Hung [9-11] modified an attached substrate with openings to allow fluid to flow between upper and lower channels. Tseng et al. [12-14] used 2D model to simulate the temperature variation and improve chip cooling under natural convection. The purpose of this study is to examine the cooling ability of the opening effect using experiment on laminar forced and natural convection. This study may help us understand the cooling ability of the opening concept on low Reynolds numbers.

S. K. Du is with the graduate institute of manufacturing technology, National Taipei University of Technology, Taiwan (e-mail: tonydu123@yahoo.com.tw).

J. C. Chang is with the Graduate Institute of Mechanical and Electrical Engineering, National Taipei University of Technology, Taiwan (e-mail: caponewilliam23@hotmail.com).

C. H. Kao is with the Department of Mechanical Engineering, Tatung University, Taiwan (e-mail: ocp2580@msn.com).

T. C. Hung is Professor with Department of Mechanical Engineering, National Taipei University of Technology, 1, Sec. 3, Chung-hsiao E. Rd., Taipei 10608, Taiwan. (Corresponding author: e-mail: tchung@ntut.edu.tw)

C. R. Lin is Professor with Department of Mechanical Engineering, National Taipei University of Technology, 1, Sec. 3, Chung-hsiao E. Rd., Taipei 10608, Taiwan. (e-mail: crlin@ntut.edu.tw)

II. Physical Model

The layout of the experiment setup is schematically shown, the major devices indicated are (1) a multi-channel temperature recorder used to measure the temperature on chip surface as shown in Fig. 1, (2) a DC power supply connected with copper dummy heater (10×10×0.2 mm^3), Corresponding density, specific heat, and thermal conductivity is 8978, 381 and 387.6, respectively. (3) two aluminum blocks (20×12×4 mm^3 and 20×12×1 mm^3) as the heater covering. In which, the density, specific heat and thermal conductivity is 2719, 871 and 202, respectively. (4) aluminum substrate (140×84×1.5 mm^3), (5) an acrylic box with 94mm width, 94mm height, and 400mm depth for forced convection, the substrate is placed on 74mm altitude as shown in Fig. 2, two DC side-blown type fans are installed at the inlet to serve as wind regime, (6) an acrylic box with 300mm width, 300mm height, and 300mm depth. As shown in Fig. 3, the substrate is placed on a platform at 110mm altitude during the natural convection model.

Fig. 4 illustrates the major experiment components of the design parameter: (1) six aluminum blocks with heater, each has an input power of 3W; (2) five aluminum substrate with different opening position and one aluminum substrate without opening used as reference case as depicted in Fig. 5, in which six different layouts of geometries are assumed; (3) a reversible aluminum substrate in order to study temperature effect of different orientation. In this study, all of the temperature measuring points in the model were marked by the symbol "#", and the cut plane for CFD simulation results is shown in Fig. 4.

CFD technology has been used for decades. FLUENT [15] could simulate conduction, convection and radiation simultaneously. Therefore, this study would employ this software package to simulate thermal hydraulics filed.

T type thermocouple is applied for measuring the temperature. A small diameter of 0.4 mm is used to measure the temperature on the chip surface in order to reduce the

interference of flow field. After calibration, the measurement error is less than 0.1K.

Fan setting and revolution is the crucial factor in making a uniform flow field under low Reynolds number. However, the major parameter is to make comparison using five different openings and the reference case which has no openings. Each opening diameter is 3mm. In forced convection, the substrate was set at the center of the acrylic box, to ensure a symmetrical flow field.

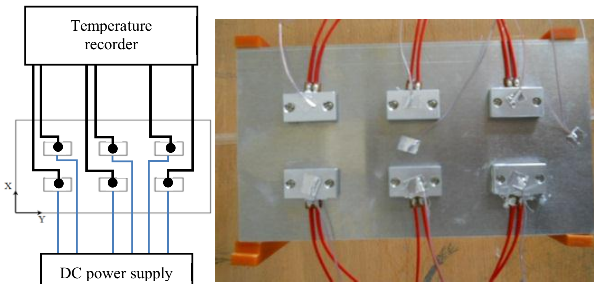

Fig. 1 Schematic diagram and test section of experiment setup

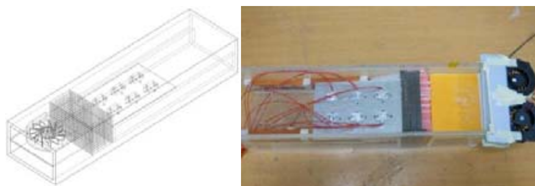

Fig. 2 Schematic and photo of forced convection model setup

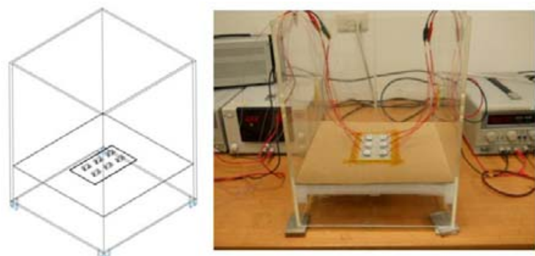

Fig. 3 Schematic and photo of natural convection model setup

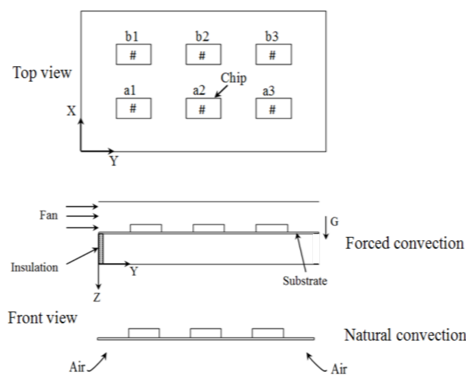

Fig. 4 Test module constitution

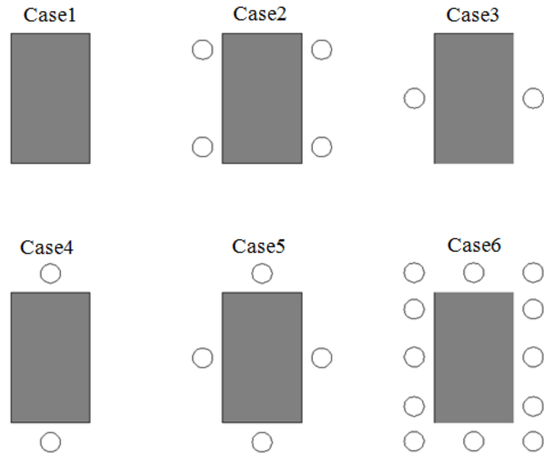

Fig. 5 Schematic diagram of opening layout

III. Mathematical and Numerical Modeling

A. Mathematical model

The steady-state governing equations on fluid and solid including conductive and convective heat transfer can be written as:

Continuity equation,

$$\frac{\partial u_i}{\partial x_j} = 0 \tag{1}$$

Momentum equation for natural convection:

$$\rho\left(u_i \frac{\partial u_j}{\partial x_i}\right) = -\frac{\partial p}{\partial x_j} + \mu\left(\frac{\partial^2 u_j}{\partial x_i}\right) - \rho\beta g\left(T - T_\infty\right)\delta_{ij} \tag{2}$$

in which, under forced convection, the last term of right hand side of Eq. 2 can be deleted.

Energy equation

$$u_i \frac{\partial T}{\partial x_j} = \alpha\left(\frac{\partial^2 T}{\partial x_j^2}\right) + \xi S \tag{3}$$

The regions with and without heat source are represented by $\xi=1$ and $\xi=0$, respectively. In this study, Boussinesq approximation is employed for the buoyant force term.

Generally speaking, radiative heat flux between two surfaces and the shape factor can be calculated by equations (4) and (5), respectively [16].

$$q''_{ij} = \sum_{j=1}^{N} A_i F_{ij}\left(J_i - J_j\right) \tag{4}$$

$$F_{ij} = \frac{1}{A_i}\int_{A_i}\int_{A_j}\frac{\cos\theta_i \cos\theta_j}{\pi r^2}dA_i dA_j \tag{5}$$

In recent years, several methods have been developed to improve the efficiency in radiative calculation for complex geometries. For instance, the employment of the finite volume method (FVM) to simulate radiation [17, 18] has been successfully applied to several problems with complex geometry [19, 20]. Meanwhile, the discrete ordinate (DO)

International Journal of Mechanical, Industrial and Aerospace Sciences
ISSN: 2517-9950
Vol:5, No:6, 2011

method, which was also extended to body-fitted geometries, has been validated by comparing with FVM [21]. In both DO model and FVM, the spatial domain is divided into a finite number of control-volume-based CFD approach. Since a simple geometry was considered in this study, the accuracy of the DO model should presumably be acceptable. This model has been validated in a previous study by Tseng et al. [12], so the DO model is employed in this study to solve the radiation transport equations. Byun et al. [22] presented a comparison of results obtained by Monte-Carlo, finite volume, and DO method for absorbing, emitting, and isotropically scattering medium that is surrounded by discretely heated irregular surfaces. They found the results of Monte-Carlo method presented the benchmark solutions within a statistical limit. While the comparative results between hand book solution and DO method provide a relative accuracy as also shown in Fig. 6, the maximum deviation is less than 8%. As a result, the DO model in this study is believed to be acceptable. Therefore, the radiative heat transfer mechanism was presented by the DO model in the following CFD work to improve the accuracy of simulation in the present study.

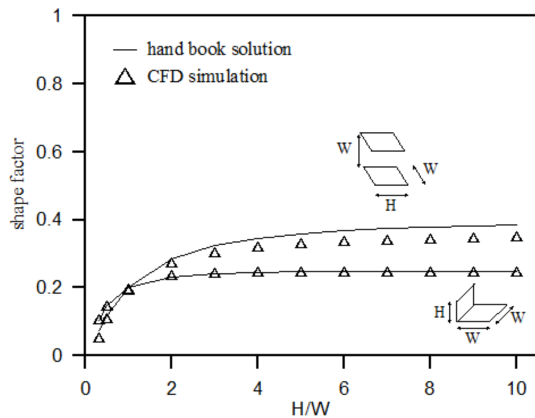

Fig. 6 Accuracy validation of the numerical DO model with theoretical values

The DO model solves the radiation transfer equation can be written as:

$$(\Omega\cdot\nabla)I(r,\Omega)=-(a_{net}+\sigma_s)I(r,\Omega)+\kappa I_b(r)+\frac{\sigma_s}{4\pi}S(r,\Omega) \quad (6)$$

in above equation, a_{net} is the net absorption coefficient; σ_s is the scattering coefficient; $\kappa = a_{net} + \sigma_s$ is the extinction coefficient. Terms $I(r,\Omega)$ and $S(r,\Omega)$ are the intensity and source term of radiation at a location of (r,Ω), respectively. $I_b(r)$ is the blackbody intensity of radiation at a location of r, and it is independent of radiation. However, the absorption and scattering effects of gas are ignored in this study due to the small density of air at 1 atm. Heat flux balance at each fluid-solid interface can be written as:

$$q''_{w,cond}=q''_{w,conv}+q''_{w,rad} \quad (7)$$

Where the thermal heat flux is expressed as:

$$q''_{w,rad}=\varepsilon\int_{n\cdot\Omega'<0}|n\cdot\Omega'|I(r_p,\Omega')d\Omega'-q_{\varepsilon,w} \quad (8)$$

The basic solution scheme employed in the current study is PISO, according to Issa et al. [23, 24]. This method employs of sequential operations at the discretized momentum, energy, and pressure-based continuity equations are solved in an alternating “predictor-corrector” fashion.

B. Numerical model

In conjugate heat transfer, it is involve two materials with highly different properties. For instance, the densities of gas and solid in the present study are about 3 orders of magnitude different. Therefore the timescales of the numerical scheme are substantially different between the gas and solid phases. When PISO is used to simulate this phenomenon, the fluid side usually requires relatively small time steps. All the governing equations were integrated over each control volume (CV), leading to a set of algebraic equations for the fluxes through the CV faces and the possible volumetric sources. The convection and diffusion fluxes of each variable at the cell faces have to be estimated based on the values of the variable at the neighboring cell center.

In conjugate heat transfer, it is involve two materials with highly different properties. For instance, the densities of gas and solid in the present study are about 3 orders of magnitude different. Therefore the timescales of the numerical scheme are substantially different between the gas and solid phases. When PISO is used to simulate this phenomenon, the fluid side usually requires relatively small time steps. All the governing equations were integrated over each control volume (CV), leading to a set of algebraic equations for the fluxes through the CV faces and the possible volumetric sources. The convection and diffusion fluxes of each variable at the cell faces have to be estimated based on the values of the variable at the neighboring cell center.

C. Boundary conditions

For forced convection, the fluid enters with a uniform velocity profile form the upper channel of one end and leaves at the other end of the plate removing the heat dissipated from the blocks. The Reynolds numbers were controlled at 2000 with a corresponding air velocity of about 1m/s. The inlet side of the lower channel is closed but the exit side is opened free to the ambient.

For the natural convection, all fluid boundaries of the simulation and experimental domain were assumed with conditions of ambient pressure (p_{in} = p_∞), and the mean environment temperature controlled at 21±1℃. Laminar flow regime is expected under Reynolds number of 2000 and natural convection in the given domain.

The acrylic box is semi-transparent medium. Partial of the radiation may be reflected, absorbed, and transmitted; thus they may induce potential deviation to CFD simulation result. Temperatures and heat flux are continuous at all fluid-solid interfaces; non-slip condition is applied at all fluid-solid interfaces to satisfy Newtonian fluid behavior. Thermal

radiation has been considered at all fluid-solid interfaces in the computational domain. The value of emissivity is considered as constant.

Table 1 Chip surface temperature of experimental measurement for Case1 (℃)

	1	2	3
a	42.9	44.6	46.8
b	43.3	44.5	46.9
T_{avg}	43.1	44.55	46.85
ΔT	23	24.45	26.75

IV. Result and Discussion

Table 1 illustrates the upper surface temperature of the chip for Case1 under forced convection. The corresponding positions of the chips are referred to Fig. 4. Due to the locally unstable air flows from the fan, small deviation may happen to the surface temperature of chip 1. It is evident from the table, when air flows through the chip surface, the temperature would be very close to the neighbor chip that is located at the same coordinate y.

In the following discussion, temperature difference ΔT is defined as:

$$\Delta T = T_{avg} - T_{\infty} \quad (9)$$

In which, T_{avg} is the mean surface temperature of the two chips with the same coordinate y normal to inlet flow from the fan; T_{∞} is the inlet temperature of the air. This definition of ΔT has been also used for the discussion of natural convection.

A. Forced convection

The variations of the temperature difference between the chip upper surface and ambient, ΔT, under forced convection with chip face upward and downward for different cases are illustrated in Figs. 7 and 8. When chips are faced downward under forced convection, the air has less ability to remove heat causing a greater ΔT. Under forced convection, the farther the chip is from entrance, the higher the surface temperature would be expected due to a thicker boundary layer.

When air flows through an opening substrate, air passes through the opening and goes into the space of another channel of the substrate due to the pressure differential near the openings beneath and above the substrate (see Fig. 9 (a)). For instance, the air of Case5 flows upward through all the openings except the opening near the exit, in which the pressure above the opening is less than that of beneath. The phenomena have been reflected in the temperature profile around the openings as shown in Fig. 9(b). From such mechanism, the air has the ability to destroy thermal boundary layer on chip periphery and lower the chip temperature. Fig. 9 (c) shows similar reason for openings amongst downward chips.

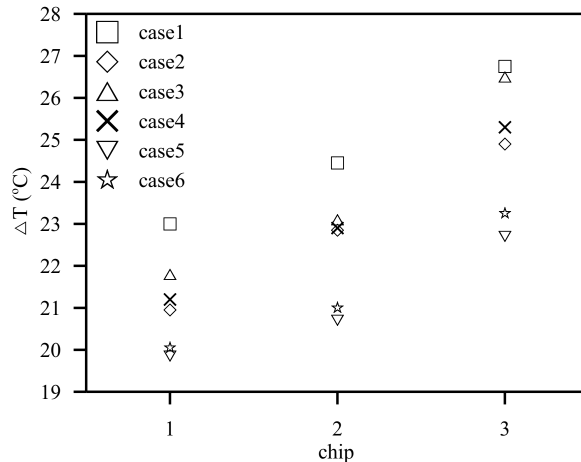

Fig. 7 Variation of the ΔT of chips under forced convection (chip face up)

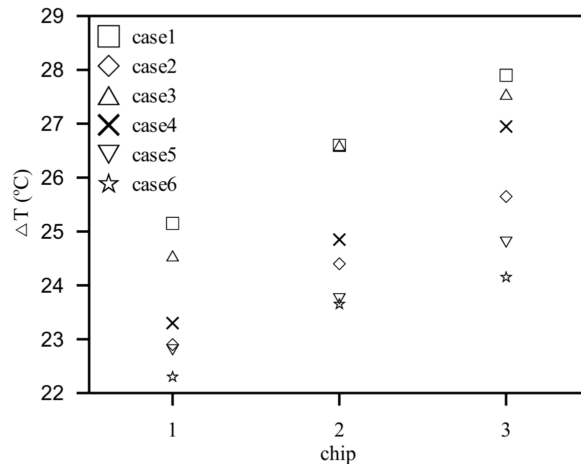

Fig. 8 Variation of the ΔT of chips under forced convection (chip face down)

Natural convection to the air is produced under the substrate via buoyancy-driven force, and thus activates more heat removal than Case1, which has no opening on the substrate. An appropriate opening would effectively enhance the overall heat transfer performance. Cases 2, 3, 4, and 5 present four distinct layouts of opening positions on the substrate, and they have performed variant heat removal ability. As main flow parallel to two opening positions (i.e., Case4),the first opening position of Case4 is prior to the chips from the entrance, and the chip surface boundary layer is disturbed via opening induced flow stream. The cold air rising up by buoyant force from lower channel combines with the stream of forced convection, so that the chip surface earns a better cooling ability to enhance cooling capability. When Case3 is compared with Case4, it shows a more obvious how the opening position has on heat removal performance. Case4 performs better than Case3 for both upward and downward of the chips because the openings of Case3 have relatively weaker effective stream to impact the chip surface. Because Case5 has both the advantages of Case3 and Case4, chips surface temperature can keep at a minimum

amongst all the cases of opening layout. Heat conduction is expected a crucial parameter in determining the effectiveness of heat removal. However, a redundant opening could reduce heat conduction effect between substrate and chip because the area for the heat conduction stream is reduced. Particularly, the substrate is made of aluminum, which has large thermal conductivity. For the reason, although Case6 may enhance heat convection mechanism, it also diminishes more heat transfer via conduction mechanism. This is expected to happen similarly for natural convection that will be discussed later in this study.

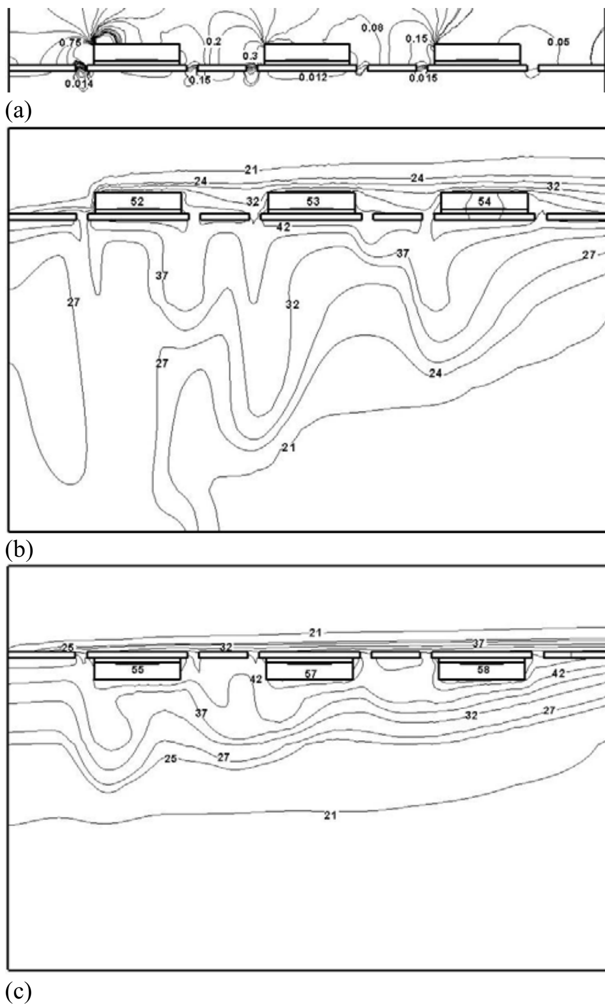

Fig. 9 Temperature distribution of y-z cut plane at the coordinate x at the center of the chips via CFD simulations under forced convection: (a) Case5, pressure distribution near the substrate (face up), (b) Case5, temperature distribution (face up), (c) Case5, temperature distribution (face down)

The measured temperatures on the surface of the chips for both orientations of upward and downward are shown in Figs. 7 and 8. For Case1 situation, the chip surface temperature cannot be effectively reduced via convection but can just be removed via the conduction of substrate and then cooled by the forced flow in the upper channel. It will therefore cause a higher surface temperature when compared with an upward orientation. As chips are under downward orientation, the number of openings is the decisive factor in heat removal ability. For instance, the result of Fig. 8 can be separated as two groups based on the mean ΔT. The cases with fewer openings have worse heat transfer ability, such as Case1, Case3 and Case4; more openings have better heat transfer ability, such as Case2, Case5 and Case6. The energy accumulated below the substrate increases the difficulty of heat removal, so the energy must pass through the openings to reduce chip temperature via air buoyant force. Case6 has the most number of openings, so the chip has the best heat removal ability when faced downward (see Fig. 8).

Since the thermal boundary layer grows from upstream in the forced convection, the last chip (i.e., chip 3) is relatively covered by thicker thermal boundary layer, which is therefore not able to provide a significant improvement in heat removal.

The mean heat transfer coefficient on the chip surface, h_m , is defined as :

$$h_m = \frac{\int_A h_A dA}{\int_A dA} \tag{10}$$

In which, A is the area of chip surface; h_A is the mean surface heat transfer coefficient for the solid-fluid interface. As shown in Fig. 10, under upward orientation, the first chip from the entrance has greater h_m but this value is decreased as the chips are far from the entrance. When the chip faces downward, air is blocked and absorbs energy in the lower channel, the last chip (i.e., chip 3) is near the outlet with the air rising up due to buoyant force. For that reason, chip 3 has higher h_m than chip 1.

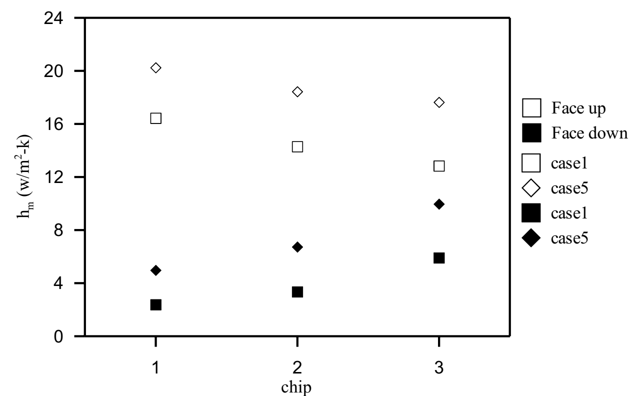

Fig. 10 Variation of chip mean heat transfer coefficient under forced convection

B. Natural convection

Under natural convection, having too many openings may also attenuate heat transfer effect. For instance, when a chip faces upward, Case3 and Case4 have better heat removal ability than Case6 as the results of ΔT shown in Fig. 11. Theoretically, the values of chip 1 and 3 should be identical because of the symmetrical layout. The reason for the unsymmetrical data is the deviation due to the measurements. In the experiment, the

opening positions of Case3 and Case5 are closer to the heater so the air around the openings has more heat absorption ability than other cases to provide a lower ΔT. It is expected that the air has greater velocity to cross the openings and effectively removes the heat from chips. Broadly speaking, the opening positions of Case2 are farther away from the heater and causes energy accumulated on the chip. Although heat conduction can help heat removal, it cannot favorably combine with convection heat transfer mechanism. Therefore, the overall value of ΔT has no obvious difference when the chip faces downward as shown in Fig. 12. The maximum enhancement in heat removal amongst all the cases is about 10% compared with that of no opening.

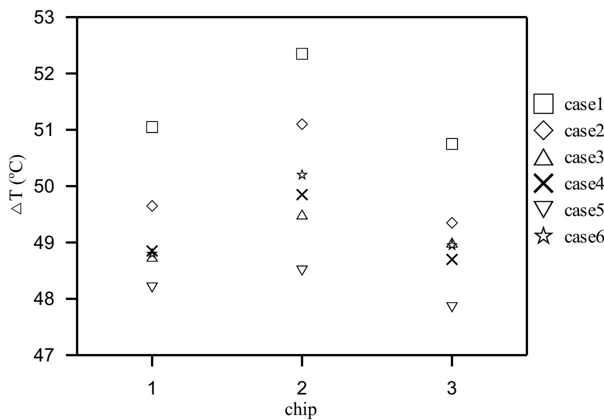

Fig. 11 Variation of the ΔT of chips under natural convection (chip face up)

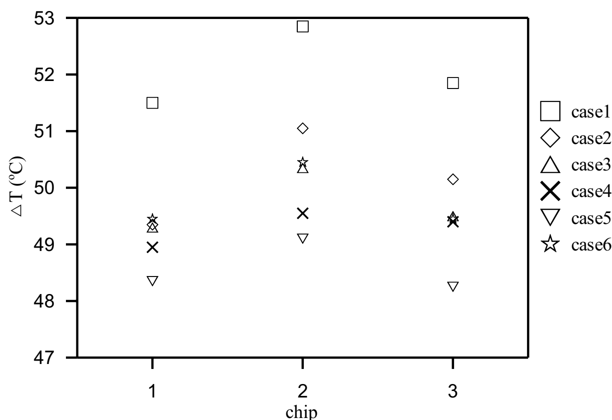

Fig. 12 Variation of the ΔT of chips under natural convection (chip face down)

In CFD simulation results, there exists some difference in values from the measured data due to the uncertainties such as the properties of materials and the setup of the experiment apparatus. The main purpose of the numerical simulations hopes to provide explanation in phenomena. Fig. 13 presents the temperature distribution of y-z cut plane at the coordinate x at the center of the chips via CFD simulations for both face up and down of Case5 under natural convection. Numerical simulations support the measurement that there exists minor difference between face up and down for Case5. It does have upward flow through all the openings around the chips but the flow strength is very limited for this case in which every chip dissipates 3W of thermal energy. As expected and as shown in the temperature profiles, center chip has thickest boundary layer. Further parametric studies for finding better performance are suggested to be done as future work.

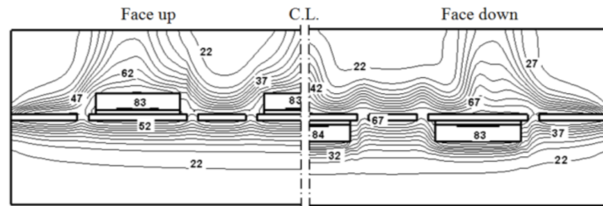

Fig. 13 Temperature distribution of y-z cut plane at the coordinate x at the center of the chips via CFD simulations for Case5 under natural convection

The results of h_m for natural convection are presented in Fig. 14. While the orientation of the chips is upward, the air is heated on the bottom substrate and flows through openings to cause a thicker boundary layer on upper surface of chips. Since Case1 does not have opening around chips, it has the least value of h_m. By comparing with the upward orientation, the downward orientation is directly impacted by induced flow with a thinner boundary layer neighboring to the chips and causing a greater h_m. As a result, comparing with the reference case, Case5 is the optimal opening design amongst all the cases studied and has the highest h_m.

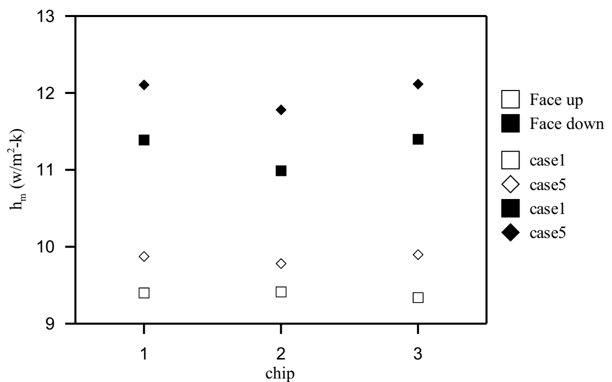

Fig. 14 Variation of chip mean heat transfer coefficient under natural convection

V. Conclusions

This study has experimentally investigated the heat transfer behavior via the use of different opening concepts on the substrate under laminar forced convection and natural convection. Coordinating with 3D numerical simulation in the present study, those results provide good candidate for further electronic package. The followings are the important findings of this study:

1) The experimental results indicated that an appropriate substrate opening layout with the chip faced upward under forced convection can reduce the maximum chip surface temperature difference. In the present study ΔT was reduced from ~27℃ (Case1) to ~23℃ (Case5).
2) This study involving experiments and CFD simulation has provided the 3D heat transfer behavior with and without opening for chip cooling under both forced and natural convection. CFD implementations provide phenomena for us to understand the variations of flow field in the simulation domains.
3) In forced convection model, chip faces upward served higher heat removal effect than downward orientation. While chip faces downward, the test model needs more opening to remove heat via buoyant force. On the other hand, when chip faces upward, too much opening may reduce heat removal capability and thus lead to an increase in the temperature of the chips.
4) In natural convection model with chip faces upward, air stream flowing through the openings blocks the cold air coming into the center of the module and hence reduces the cooling ability to the surface of the chip. While chips are facing downward, cold air flows directly and impacts main chip surface and induce stronger cooling ability.
5) Through a parametric study such as the one described, future substrate design can consider this opening concept to reduce the temperature of the chips.

NOMENCLATURE

A area
a absorption coefficient
C_p specific heat
F shape factor
g gravity
h_m mean surface heat transfer coefficient
I radiation intensity
J the definition of radiosity, $J_i \equiv \epsilon_i E_{bi} + (1-\epsilon_i)G_i$
k thermal conductivity
n real component of the complex index of refraction, accuracy of the DOM model
N_u Nusselt number
q'' heat flux
r Cartesian coordinate vector
S source term
T temperature
u i-component velocity
x i-component coordinate

Greek symbols
α thermal diffusivity
β thermal expansion coefficient
ε surface emissivity
γ Cartesian coordinate vector
κ extinction coefficient
μ dynamic viscosity
σ Stefan-Boltzmann constant
σ_s scattering coefficient
δ_{ij} delta function=1 when i = j and =0 when i ≠ j
ξ 1 and 0 for solid region with and without source, respectively
ρ density
Ω ordinate direction vector

Subscripts
b blackbody
$cond$ conduction
$conv$ convection
i,j surface index
m mean value
net net value
rad radiation
s solid
w wall
∞ surrounding

REFERENCE

[1] A. Bar-Cohen, A. D. Kraus, and S. F. Davidson, "Thermal Frontiers in the Design and Packaging of Microelectronic Equipment," *Eng*., vol. 105, no. 6, 1983, pp. 53–59.
[2] L. T. Yeh, "Review of Heat Transfer Technologies in Electronic Equipment," *ASME J. Electron. Packaging*, vol. 117, 1995, pp. 333-339.
[3] F. P. Incropera, "Convection Heat Transfer in electronic equipment," *ASME J. Heat Transfer*, vol. 110, 1988, pp. 1097-1107.
[4] E. M. Sparrow, J. E. Niethammaer and A. Chaboki, "Heat transfer and pressure drop characteristics of arrays of rectangular modules encountered in electronics equipment," *International J. Heat and Mass Transfer*, vol. 25, no. 7, 1982, pp. 961-973.
[5] E. M. Sparrow, S. B. Verumi and D. S. Kadle, "Enhanced and local heat transfer, pressure drop, and flow visualization for arrays of block-like electronic components," *International J. Heat and Mass Transfer*, vol. 26, no. 5, 1983, pp. 689-699.
[6] E. M. Sparrow, A. A. Yanezmoreno and D. R. Otis, "Convective heat transfer response to height difference in an array of block-like electronic equipment," *International J. Heat and Mass Transfer*, vol. 27, no. 3, 1984, pp. 469-473.
[7] R. J. Moffat, A. Ortega and D. E. Arvizu, "Cooling electronic components: forced convection experiments with an air cooled array," *Heat Transfer in Electronic Equipment, ASME HTD*, vol. 48, 1985, pp. 15.
[8] Y. Asako and M. Faghri, "Three-dimensional heat transfer and fluid flow analysis of rectangular blocks encountered in electronic equipment," *Numer. Heat Transfer*, vol.13, 1988, pp. 481.
[9] T. C. Hung, S. K. Wang and F. P. Tsai, "Simulation of passively conjugate heat transfer across an array of volumetric heat sources," *J. Communications in Numerical Methods in Engineering,* vol. 13, 1997, pp. 855-866.
[10] T. C. Hung and C. S. Fu, "Conjugate heat transfer analysis for the passive enhancement of electronic cooling through geometric modification in a mixed convection domain," *Numer. Heat Transfer-Part A*, vol. 35, no. 5, 1999, pp. 519-535.
[11] T. C. Hung, "A conceptual desing of thermal modeling for efficiently cooling an array of heated devices under low Reynolds numbers," *Numer. Heat Transfer-Part A*, vol. 39, 2001, pp. 361-382.
[12] Y. S. Tseng, B. S. Bai and T.C. Hung, "Effects of thermal radiation on modified PCB Geometry under natural convection," *Numer. Heat Transfer-Part A*, vol. 51, 2007, pp. 195-210.
[13] Y. S. Tseng, T. C. Hung and B. S. Bai, "Enhancement of cooling characteristics for electronic cooling by modifying substrate under natural convection," *ASME J. Electronic Packing*, vol. 130, no. 1, 2008, pp. 11006.1-11006.8.
[14] Y. S. Tseng, H. H. Fu, T. C. Hung and B. S. Bai, "An optimal parametric design to improve chip cooling," *International J. Applied Thermal Engineering*, vol. 27, 2007, pp. 1823-1831.
[15] ANSYS Inc., *FLUENT V12 User's Guide*. 2009.
[16] Incropera, F. P., Dewitt, D. P., Bergman, T. L., Lavine, A. S., *Introduction to heat transfer*, 5th ed., New York:Wiley, 2005, ch. 13, pp. 773 and 785.

[17] Chui, E.H., Raithby, G.D., "Computation of radiant heat transfer on a non-orthogonal mesh using the finite-volume method," *Numer. Heat Transfer-Part B*, vol. 23, 1993, pp. 269–288.
[18] Chai, J.C., Lee, H.S., Patanker, S.V., "Finite volume radiative heat transfer procedure for irregular geometries," *J. Thermophys. Heat Transfer*, vol. 19, no. 3, 1995, pp. 410–415.
[19] Kim, M.Y., Baek, S.W., "Numerical analysis of conduction, convection, and radiation in a gradually expanding channel," *Numer. Heat Transfer-Part A*, vol 29, 1996, pp. 725–740.
[20] Baek, S.W., Kim, M.Y., "Nonorthogonal finite-volume solutions of radiative heat transfer in a three-dimensional enclosure," *Numer. Heat Transfer-Part B*, vol 34, pp. 419–437.
[21] Liu, J.S., Shang, H.M., Chen, Y.S., Wang, T.S., "Prediction of radiative transfer in general body-fitted coordinates," *Numer. Heat Transfer-Part B*, vol. 31, 1997, pp. 423–439.
[22] Byun, D. Y. Baek, S. W., Kim, M. Y., "Thermal radiation in a discretely heated irregular geometry using the Monte-Carlo, finite volume, and modified discrete ordinates interpolation method," *Numer. Heat transfer-Part A*, vol. 37, 2000, pp. 1-18.
[23] R. I. Issa, A. D. Gosman, and A. P. Watkins, "The Computation of Compressible and incompressible recirculating flows by a non-iterative Implicit Scheme," *J. Comput. Phys*., vol. 62, 1986, pp. 66-82.
[24] R. I. Issa, B. Ahmadi-Befrui, K. R. Beshay, and A. D. Gosman, "Solution of the Implicit Discretized Reacting Flow Equations by Operator-Splitting," J. Comput. Phys., vol. 93, 1991, pp. 388-410.